Electronic Supplementary Material (ESI) for Nanoscale.
This journal is © The Royal Society of Chemistry 2019

Supporting Information

Magnetization Reversal Mechanism in Electrospun Tubular Nickel Ferrite: A Chain-of-Rings Model for Symmetric Fanning

Junli Zhang[a], Shimeng Zhu[a], Jun Ming[b], Liang Qiao[a], Fashen Li[a], Abdul Karim[a,c], Yong Peng[a]*, Jiecai Fu[a]*

[a]Key Laboratory of Magnetism and Magnetic Materials of Ministry of Education, School of Physical Science and Technology, Lanzhou University, Lanzhou 730000, P. R. China

[b]State Key Laboratory of Rare Earth Resource Utilization, Changchun Institute of Applied Chemistry, Chinese Academy of Sciences, Changchun 130022, P. R. China

[c]Department of Physics, Karakorum International University Gilgit-Baltistan, Gilgit 15100, Pakistan

E-mail: pengy@lzu.edu.cn; fujc@lzu.edu.cn

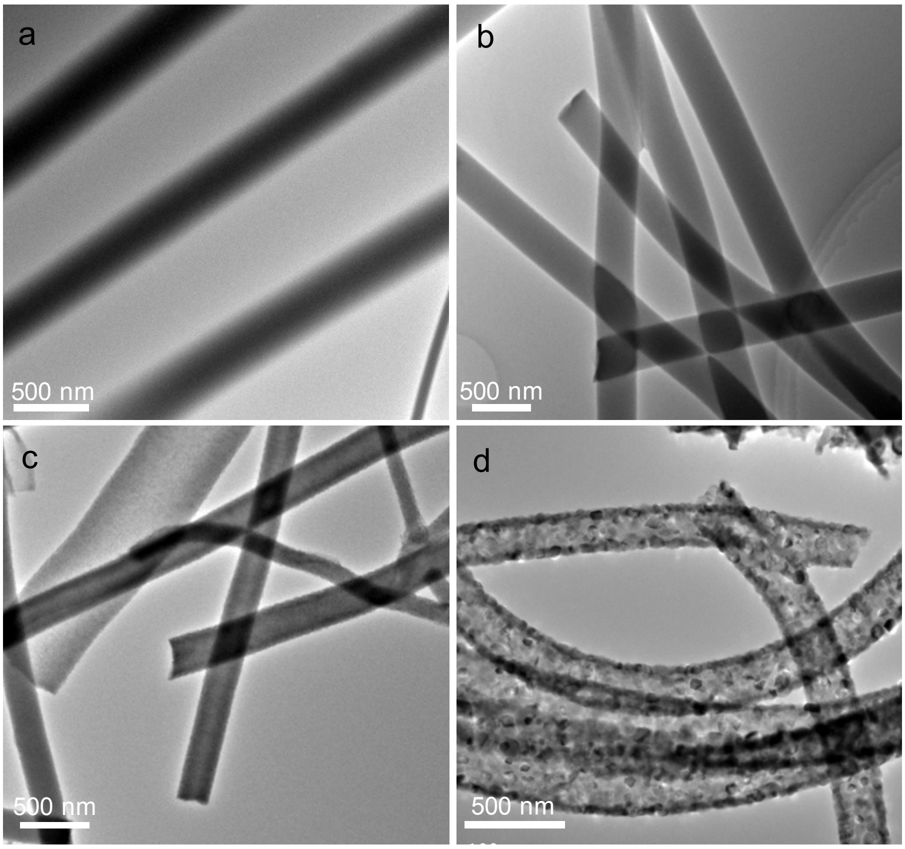

Figure S1. TEM micrographs of electrospun $NiFe_2O_4$ nanofibers evolutionary process after calcination at different temperature, indicating the diameter of nanofibre decreased as increasing the calcination temperature (due to the removal of PVP): (a) 100 °C; (b) 300 °C; (c) 400 °C; (d) 600 °C.

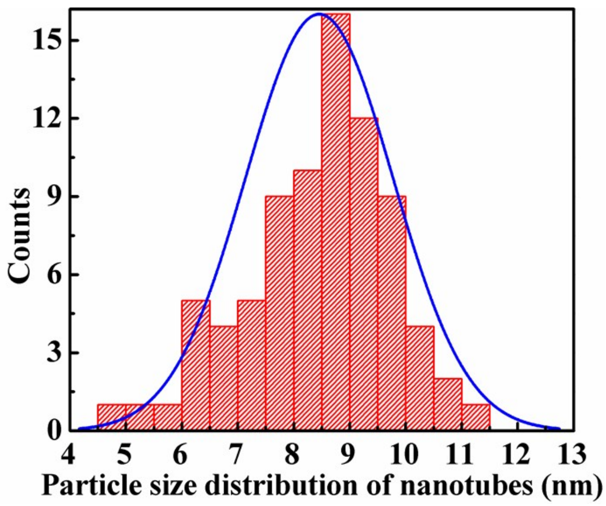

Figure S2. Size distribution of nanoparticles (*i.e.*, building blocks) within the $NiFe_2O_4$ nanotubes.

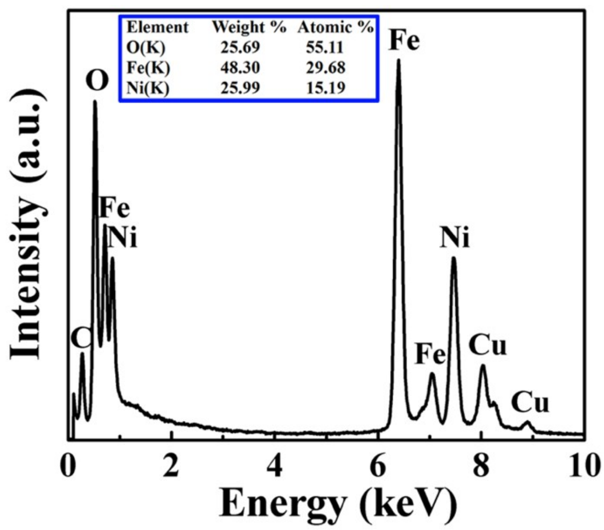

Figure S3. EDX spectrum of $NiFe_2O_4$ nanotubes.

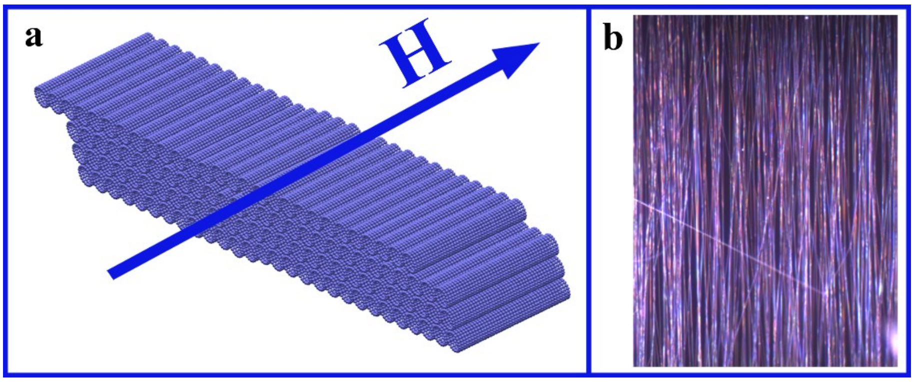

Figure S4. (a) Schematic illustration of VSM measurement; (b) Optical micrograph of a uniaxially aligned $NiFe_2O_4$ nanotubes array that was collected on a silicon wafer.

Note 1

The demagnetizing factor (N_z) of $NiFe_2O_4$ nanotubes can be calculated by [1]:

$$N_z = \frac{2R}{L(1-\beta^2)} \int_0^{\infty} \frac{dq}{q^2} (J_1(q) - \beta J_1(\beta q))^2 \ (1 - e^{-q\frac{L}{R}}) \tag{1}$$

$$\beta = b/R \tag{2}$$

where R, b and L are outer radius, inner radius and length of nanotubes (**Figure S5**), respectively. $J_1(q)$ are Bessel functions of the first kind. Then, the demagnetizing factor of the prepared $NiFe_2O_4$ nanotubes is calculated to be 0.0035, which is close to zero.

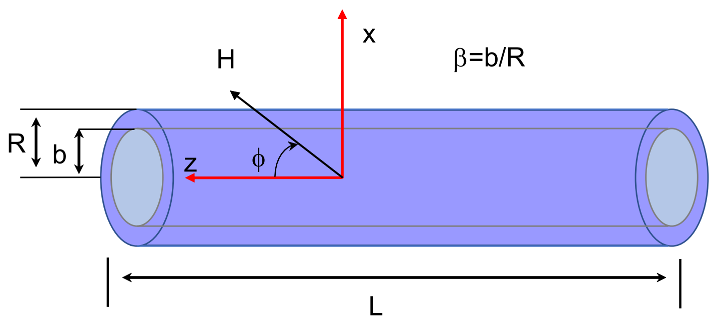

Figure S5. Geometrical parameters of $NiFe_2O_4$ nanotube.

Note 2

The total energy of the symmetric funning mode under an external magnetic field can be formulated as [2]:

$$E_n = 20n\, L_n \frac{\mu^2}{a^3}\left(1 - 3cos^2\theta\right) + 20n\, M_n \frac{\mu^2}{a^3}\left(cos2\theta - 3cos^2\theta\right)$$

$$+ \sum_{N=1}^{9} 20nO_n \frac{\mu^2}{a^3}\left(1 - 3cos^2\theta\right) + 10nO_{10}\frac{\mu^2}{a^3}\left(1 - 3cos^2\theta\right)$$

$$+ \sum_{N=1}^{9} 20n\, P_n \frac{\mu^2}{a^3}\left(cos2\theta - 3cos^2\theta\right) + 10nP_{10}\frac{\mu^2}{a^3}\left(cos2\theta - 3cos^2\theta\right)$$

$$+ 20n\mu Hcos\theta, \tag{3}$$

And the total energy of the parallel rotation mode can be expressed as:

$$E_p = 20n\, K_n \frac{\mu^2}{a^3}\left(1 - 3cos^2\theta\right) + \sum_{N=1}^{9} 20nQ_n \frac{\mu^2}{a^3}\left(1 - 3cos^2\theta\right)$$

$$+ 10nQ_{10}\frac{\mu^2}{a^3}\left(1 - 3cos^2\theta\right) + 20n\mu Hcos\theta \quad , \tag{4}$$

The relevant parameters can be summarized as below:

$$K_n = \sum_{j=1}^{n} \frac{n-j}{nj^3} \quad , \tag{5}$$

$$Q_n = \sum_{j=0}^{n-1} \frac{n-j}{n\left(\sqrt{\left(\frac{d_N}{a}\right)^2 + j^2}\right)^3} \quad , \tag{6}$$

$$K_n = L_n + M_n \, , \tag{7}$$

$$Q_n = O_n + P_n \, , \tag{8}$$

where, $\cos 2\theta < 1$ and $\cos\gamma_n = -\cos\varphi_n$, thus $E_n < E_p$."

Note 3

Note that the interaction between the nanotubes can be neglected. This is because the magnetostatic energy is inversely proportioned to d^3 (wherein the d is the distance between dipoles), then the magnetostatic interaction energy can be decreased significantly as increasing the inter-dipoles distance. Herein, we analyze the total energy of two neighboring nanotubes under an external magnetic field to confirm the neglected contribution from the tube-tube interactions (**Figure S6**):

$$E_n = 40n\,L_n\frac{\mu^2}{a^3}(1-3cos^2\theta) + 40n\,M_n\frac{\mu^2}{a^3}(cos2\theta - 3cos^2\theta)$$

$$+\sum_{N=1}^{9} 40nO_n\frac{\mu^2}{a^3}(1-3cos^2\theta) + 20nO_{10}\frac{\mu^2}{a^3}(1-3cos^2\theta)$$

$$+\sum_{N=1}^{9} 40n\,P_n\frac{\mu^2}{a^3}(cos2\theta - 3cos^2\theta) + 20nP_{10}\frac{\mu^2}{a^3}(cos2\theta - 3cos^2\theta)$$

$$+ n\,L_n\frac{\mu^2}{a^3}(1-3cos^2\theta) + 40n\,M_n\frac{\mu^2}{a^3}(cos2\theta - 3cos^2\theta)$$

$$+ 2n\,L_n\frac{\mu^2}{(2a)^3}(1-3cos^2\theta) + 2n\,M_n\frac{\mu^2}{(2a)^3}(cos2\theta - 3cos^2\theta)$$

$$+ \;\ldots + nR_n\frac{\mu^2}{(a)^3}(1-3cos^2\theta) + n\,S_n\frac{\mu^2}{(a)^3}(cos2\theta - 3cos^2\theta)$$

$$+ \;10nT_n\frac{\mu^2}{(a)^3}(1-3cos^2\theta) + 10n\,W_n\frac{\mu^2}{(a)^3}(cos2\theta - 3cos^2\theta)$$

$$+ \;10nV_n\frac{\mu^2}{(a)^3}(1-3cos^2\theta) + 10n\,U_n\frac{\mu^2}{(a)^3}(cos2\theta - 3cos^2\theta)$$

$$+ 40n\mu Hcos\theta$$

(9)

wherein the relevant parameters can be summarized as:

$$R_n = \sum_{j=0}^{\frac{n-1}{2} < n \le \frac{n}{2}} \frac{n-2j}{n(\sqrt{\left(\frac{2R}{a}\right)^2 + (2j)^2})^3} \tag{10}$$

$$S_n = \sum_{j=1}^{\frac{n-1}{2} < n \le \frac{n+1}{2}} \frac{n-2j}{n(\sqrt{\left(\frac{2R}{a}\right)^2 + (2j-1)^2})^3} \tag{11}$$

$$T_n = \sum_{N=1}^{5} \sum_{j=0}^{\frac{n-1}{2} < n \le \frac{n}{2}} \frac{n-2j}{n(\sqrt{\left(\frac{2R+0.1NR}{a}\right)^2 + (0.1NR)^2 + (2j)^2})^3}, \tag{12}$$

$$W_n = \sum_{j=1}^{\frac{n-1}{2} < n \le \frac{n+1}{2}} \frac{n-2j}{n(\sqrt{\left(\frac{2R+0.1NR}{a}\right)^2 + (0.1NR)^2 + (2j-1)^2})^3}, \tag{13}$$

$$V_n = \sum_{N=1}^{5} \sum_{j=0}^{\frac{n-1}{2} < n \le \frac{n}{2}} \frac{n-2j}{n(\sqrt{\left(\frac{3R+0.1NR}{a}\right)^2 + \quad (0.5R-0.1NR) + (2j)^2})^3}, \tag{12}$$

$$U_n = \sum_{j=1}^{\frac{n-1}{2} < n \le \frac{n+1}{2}} \frac{n-2j}{n(\sqrt{\left(\frac{3R+0.1NR}{a}\right)^2 + \quad (0.5R-0.1NR) + (2j)^2})^3}, \tag{13}$$

Where *2R=20a* is the diameter of nanotubes. We find that variation of the magnetostatic energy is less than 10% (about 8%) when we consider tube-tubes interaction (terms 7-16). This result confirms that the tube-tubes interaction can be neglected.”

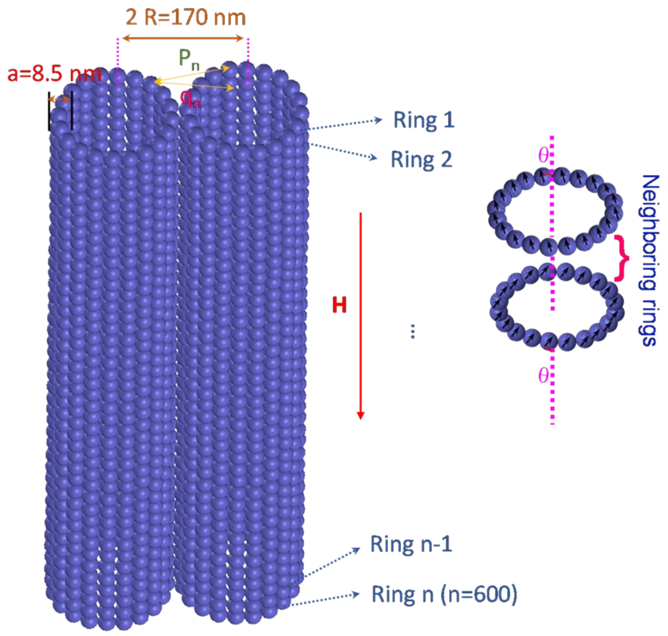

Figure S6. Schematic illustration of the two neighboring nanotubes when the applied magnetic field is parallel to the nanotubes.

Note 4

The energy of the system achieves the minimum value when the magnetic field reaches the coercive field. Thus, the theoretical coercivity can be obtained by calculating the equilibrium values of γ and ϕ as varying the values of the field H at the fixed ψ, where the first derivation for the energy of the system is equal to zero:

$$\frac{\partial E_n}{\partial \phi} = 0, \tag{14}$$

$$\frac{\partial E_n}{\partial \gamma} = \frac{\partial E_m}{\partial \gamma} + \frac{\partial E_f}{\partial \gamma} = 0, \tag{15}$$

Which can be expanded respectively as below:

$$\frac{\partial E_n}{\partial \phi} = \left(60nK_n + \sum_{N=1}^{9} 60nQ_n + 30nQ_{10}\right)\frac{\mu^2}{a^3}(\sin^2 \psi \sin^2 \gamma \sin 2\phi + 2sin\psi cos\psi \sin \gamma c \\ - (40nM_n + \sum_{N=1}^{9} 40nP_n + 20nP_{10})\frac{\mu^2}{a^3}\sin^2 \gamma \sin 2\phi = 0 \tag{16}$$

$$\frac{\partial E_n}{\partial \gamma} = 2\left(60nK_n + \sum_{N=1}^{9} 60nR_n + 30nR_{10}\right)\frac{\mu^2}{a^3}(\sin^2 \psi \cos^2 \phi \sin \gamma cos\gamma + sin\psi cos\psi cc \\ - \left(40nM_n + \sum_{N=1}^{9} 40nP_n + 20nP_{10}\right)\frac{\mu^2}{a^3}\sin \gamma cos\gamma(\cos 2\phi - 1) \\ - 20n\mu H sin\gamma = 0 \tag{17}$$

Then, the roots of Eq.16 can be calculated as below:

$$sin\phi = 0, \quad \phi = 0, \pi \tag{18}$$

and/or

$$\left[\left(60nK_n+\sum_{N=1}^{9}60nQ_n+30nQ_{10}\right)\sin^2\psi-\left(40nM_n+\sum_{N=1}^{9}40nP_n+20nP_{10}\right)\right]\frac{\mu^2}{a^3}sin\,\gamma cos\phi=\frac{1}{2}\left(60nK_n+\sum_{N=1}^{9}60nQ_n+30nQ_{10}\right)\frac{\mu^2}{a^3}sin2\psi cosr \tag{19}$$

In this way, the relation between γ and ϕ can be obtained from Eq.19 as below:

$$cos\phi=A(\psi)cot\gamma \tag{20}$$

where

$$A(\psi)=\frac{3\left(K_n+\sum_{N=1}^{9}Q_n+\frac{Q_{10}}{2}\right)\sin 2\psi}{6\left(K_n+\sum_{N=1}^{9}Q_n+\frac{Q_{10}}{2}\right)sin^2\psi-4(M_n+\sum_{N=1}^{9}P_n+\frac{P_{10}}{2})} \tag{21}$$

In addition, the second derivation for the energy of the system is higher than zero when the energy of the system is at the minimum value, which can be described as below:

$$\frac{\partial^2E_n}{\partial\phi^2}=\left(60nK_n+\sum_{N=1}^{9}60nQ_n+30nQ_{10}\right)\frac{\mu^2}{a^3}(2\sin^2\psi\sin^2\gamma\cos 2\phi+2sin\psi cos\psi\sin\ldots-2\left(40nM_n+\sum_{N=1}^{9}40nP_n+20nP_{10}\right)\frac{\mu^2}{a^3}\sin^2\gamma\cos 2\phi>0 \tag{22}$$

Then, the Eq. 22 can be solved in three different conditions (I, II, III) when the angle ϕ *is equal to* 0, $acos[A(\psi)cot\gamma]$ and π, respectively.

(I) when $\phi=0$,

The Eq. 22 can be simplified to

$$[2\sin^2\psi\left(60nK_n+\sum_{N=1}^{9}60nQ_n+30nQ_{10}\right)sin^2\psi-2\left(40nM_n+\sum_{N=1}^{9}40nP_n+20nP_{10}\right)]\frac{\mu^2}{a^3}sin^2\gamma+\left(60nK_n+\sum_{N=1}^{9}60nQ_n+30nQ_{10}\right)\frac{\mu^2}{a^3}sin2\psi sin\gamma cos\gamma>0 \tag{23}$$

The angle γ is given by:

$$0<\gamma\leq atanA(\psi) \tag{24}$$

(II) when $\phi=acos[A(\psi)cot\gamma]$

The Eq. 22 can be simplified to

$$[2\sin^2\psi\left(60nK_n+\sum_{N=1}^{9}60nQ_n+30nQ_{10}\right)sin^2\psi-2\left(40nM_n+\sum_{N=1}^{9}40nP_n+20nP_{10}\right)]\frac{\mu^2}{a^3}sin^2\gamma cos2\phi+\left(60nK_n+\sum_{N=1}^{9}60nQ_n+30nQ_{10}\right)\frac{\mu^2}{a^3}sin2\psi sin\gamma cos\gamma cos\phi>0$$

(25)

Then the Eq. 25 can be simplified to

$$tan\gamma>-A(\psi)\frac{\cos\phi}{\cos 2\phi}=\frac{[A(\psi)]^2cot\gamma}{1-2[A(\psi)]^2cot^2\gamma} \tag{26}$$

Thus,

$$|tan\gamma|>A(\psi) \tag{27}$$

(III) When $\phi=\pi$,

$$[2\sin^2 \psi\left(60nK_n+\sum_{N=1}^{9}60nQ_n+30nQ_{10}\right)sin^2\psi-2\left(40nM_n+\sum_{N=1}^{9}40nP_n+20nP_{10}\right)]\frac{\mu^2}{a^3}sin^2\gamma+\left(60nK_n+\sum_{N=1}^{9}60nQ_n+30nQ_{10}\right)\frac{\mu^2}{a^3}sin2\psi sin\gamma cos\gamma > 0 \quad (28)$$

The angle γ is then given by:

$$acot\left(-\frac{1}{A(\psi)}\right)\leq\gamma<\pi \quad (29)$$

The fanning mechanism happens in the range II, and this range decreases as increasing ψ until $\psi\geq\psi_0$. Then, the magnetization reversal process is completed by the coherent rotation mechanism, because there is no solution for Eq.20 when $\psi\geq\psi_0$. Thus, the polar angle $\gamma=atanA(\psi)$ can be considered as the inflection point from the coherent rotation to the fanning reversal. In addition, the Eq.20 was substituted into Eq.17 for exploring the relations between the coercivity and the ψ in fanning reversal mechanism. The first order differential equation is then described as below:

$$\frac{\partial E_n}{\partial\gamma}=-2\left(60nK_n+\sum_{N=1}^{9}60nQ_n+30nQ_{10}\right)\frac{\mu^2}{a^3}\left(\sin^2\psi A(\psi)^2cot^2\gamma\sin\gamma cos\gamma+sin\psi cos\psi cos2\gamma A(\psi\right.$$
$$+2\left(40nM_n+\sum_{N=1}^{9}40nP_n+20nP_{10}\right)\frac{\mu^2}{a^3}\sin\gamma cos\gamma\left(A(\psi)^2cot^2\gamma-1\right)-20n\mu Hsin\gamma=0 \quad (30)$$

wherein,

$$-\frac{\partial E_f}{\partial\gamma}=20n\mu Hsin\gamma, \quad (31)$$

$$\frac{\partial E_m}{\partial \gamma} = 60n\frac{\mu^2}{a^3}\left(K_n + \sum_{N=1}^{9} Q_n + \frac{Q_{10}}{2}\right)[A(\psi)cot^2\gamma sin\gamma cos\gamma \sin 2\psi - \sin 2\psi cos2\gamma A(\psi)c$$
$$-\left(40M_n + \sum_{N=1}^{9} 40P_n + 20P_{10}\right)\frac{\mu^2}{a^3}sin2\gamma \qquad (32)$$

Then, the solution for γ is obtained by plotting the curves of γ *vs.* $-\frac{\partial E_f}{\partial \gamma}$ and γ *vs.* $\frac{\partial E_m}{\partial \gamma}$ respectively, where the point of intersection is the solution for γ. Note that the values of H and ψ were fixed in the discussion. Thus, we can see the curves and the point of intersection when H = 250 Oe, or H = 300 Oe and ψ=30°, as shown in **Figure S7**. Finally, the formatted hysteresis loop (cosγ *versus* H) and the coercivity versus ψ can be obtained for the fanning reversal (Figure 4c)."

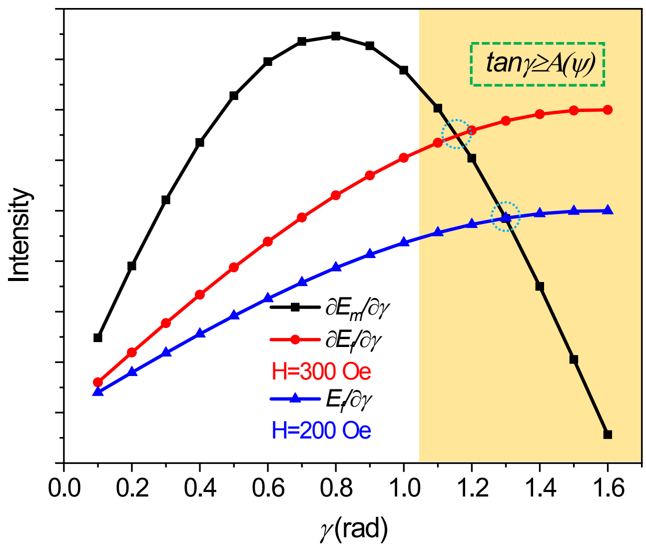

Figure S7. Plotted curves of γ *vs.* $-\frac{\partial E_f}{\partial \gamma}$ and γ *vs.* $\frac{\partial E_m}{\partial \gamma}$ when H = 250 Oe, or H = 300 Oe and ψ=30°.

Note 5

The magnetocrystalline anisotropy energy of cubic system can be expressed by:

$$E_k = K_1\left({\alpha_1}^2{\alpha_2}^2 + {\alpha_2}^2{\alpha_3}^2 + {\alpha_3}^2{\alpha_1}^2\right), \tag{33}$$

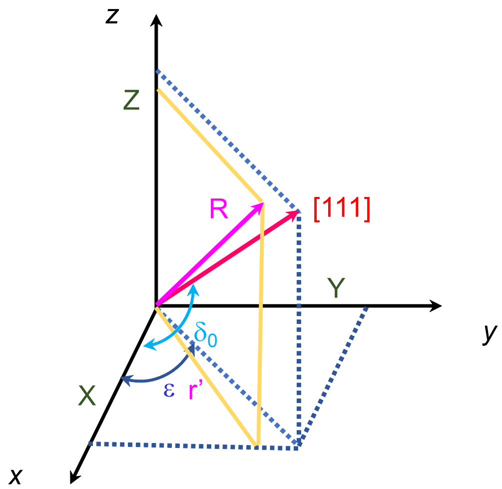

Figure S8. Direction cosines of magnetization in dipolar coordinates.

where α_1, α_2 and α_3 are direction cosines of the magnetic moment with respect to the cubic *a*-, *b*- and *c*-axes, respectively. It is well known that the [111] direction is one easy axis in the $NiFe_2O_4$ as its magnetocrystalline anisotropy constant K_1<0. Thus, the angle between [111] direction and *x*-axis (*i.e.* δ_0) equal to $cos^{-1}\frac{1}{\sqrt{3}}$ and $\varepsilon = 45°$ (**Figure S8**). If the magnetic moment deviates from the [111] direction for a small angle δ (**Figure S8**), the direction cosines can be rewritten as:

$$\alpha_1 = \frac{1}{\sqrt{2}}\sin\left(\delta_0 + \delta\right) \tag{34}$$

$$\alpha_2 = \frac{1}{\sqrt{2}}\sin\left(\delta_0 + \delta\right) \tag{35}$$

$$\alpha_3 = cos(\delta_0 + \delta) \tag{36}$$

According to Eq.31-32, the Eq.30 is converted as

$$E_k = K\left[sin^2(\delta_0 + \delta\right) - \frac{3}{4}sin^4(\delta_0 + \delta)] \tag{37}$$

As the angle between magnetic moment and [111] direction is small, the anisotropy energy (Eq.34) reduces to

$$E_k = \frac{K_1}{3} - \frac{2}{3}K_1\delta^2 \tag{38}$$

where the first term is the energy in easy axis direction, thus we have

$$E = -\frac{2}{3}K_1\delta^2 = \frac{J_s H_k}{2}\delta^2 \tag{39}$$

where K_1 and J_s are the magnetocrystalline anisotropy constant and saturation magnetic dipole moment per unit volume. Thus effective magnetocrystalline anisotropy field in $NiFe_2O_4$ given by [3]:

$$H_k = -\frac{4K_1}{3M_s}, \tag{40}$$

where M_s is the saturation magnetization. Then, the effective anisotropy field of $NiFe_2O_4$ is calculated to be 518 Oe, according to the **Eq. 40.**

References

[1] J. Escrig, M. Daub, P. Landeros, K. Nielsch, D. Altbir, *Nanotechnology* **2007**, *18*, 445706.

[2] I. S. Jacobs, C. P. Bean, *Phys. Rev.* **1955**, *100*, 1060-1067.

[3] A. Globus, P. Duplex, M. Guyot, *Ieee. T. Magn.* **1971**, *7*, 617-622.